

Article

Orbital Transfers in a Binary Asteroid System Considering Flattening of the Bodies and Solar Radiation Pressure

L. B. T. Santos ^{1,†}, V. Y. Razoumny ^{2,*} , V. M. Gomes ^{3,†}  and A. F. B. A. Prado ^{2,4,*}, [†]¹ University of Pernambuco (UPE), Recife 50720-001, Brazil; leonardo.torres@upe.br² Peoples' Friendship University of Russia Named After Patrice Lumumba (RUDN University), 6, Miklukho-Maklaya Str., 117198 Moscow, Russia³ School of Engineering and Sciences, São Paulo State University (UNESP), São Paulo 01049-010, Brazil; vivian.gomes@unesp.br⁴ National Institute for Space Research (INPE), São José dos Campos 12227-010, Brazil

* Correspondence: razoumny-vyu@rudn.ru (V.Y.R.); antonio.prado@inpe.br (A.F.B.A.P.)

† These authors contributed equally to this work.

Abstract: This paper aims to investigate the effects of asteroid size and shape and solar radiation pressure in the trajectories of a spacecraft in transfers between the collinear equilibrium points of a binary non-spherical asteroid system. As an example, we consider the physical and orbital characteristics of the asteroid system 2001SN263. The goal is not to study this system in detail, but to use its parameters to search for transfers considering elongated bodies for the asteroids and compare the results with the solutions obtained when modeling the bodies as point masses. For the propulsion system, bi-impulsive transfers were investigated. In a system composed of asteroids, it is important to take into account the elongation of the asteroids, particularly the body with the most irregular shape, as this has been shown to change the optimal transfer trajectories. By incorporating solar radiation pressure and the size of the bodies into the dynamics, solutions with both lower and higher fuel consumption can be identified. Although the irregular shape and radiation pressure were not used as controls, their effects on the transfers are analyzed. For a system of small bodies, such as an asteroid system, it is very important to consider these perturbations to ensure that the spacecraft will reach the desired point.

Keywords: astrodynamics; orbital transfers; asteroids; orbital perturbations



Citation: Santos, L.B.T.; Razoumny, V.Y.; Gomes, V.M.; Prado, A.F.B.A. Orbital Transfers in a Binary Asteroid System Considering Flattening of the Bodies and Solar Radiation Pressure. *Aerospace* **2024**, *11*, 1058. <https://doi.org/10.3390/aerospace11121058>

Academic Editor: Shuang Li

Received: 26 October 2024

Revised: 20 December 2024

Accepted: 22 December 2024

Published: 23 December 2024



Copyright: © 2024 by the authors. Licensee MDPI, Basel, Switzerland. This article is an open access article distributed under the terms and conditions of the Creative Commons Attribution (CC BY) license (<https://creativecommons.org/licenses/by/4.0/>).

1. Introduction

A great interest has been observed in recent years in the exploration of small bodies in the solar system [1]. In 1994, a moon orbiting an asteroid was observed for the first time. Until that moment, it was believed that asteroids and comets were solitary bodies. After that, asteroids with rings were found, as well as several other systems of double and triple asteroids [2,3]. It is also important to remember that spacecraft have been sent to explore asteroids and comets only in the 21st century. The American spacecraft NEAR Shoemaker landed on the asteroid Eros in 2000 and a Japanese spacecraft called Hayabusa analyzed data and collected materials from the asteroid Itokawa, in 2003. In order to collect data to better understand the origin and formation of the solar system, an American spacecraft called Dawn orbited the asteroid Vesta in 2012. A mission launched by the ESA (European Space Agency), the ROSETTA Mission, achieved a historic milestone: a successful flight with the innovative soft landing of the Philae spacecraft on the comet 67P/Churyumov-Gerasimenko in November 2013 [2]. These missions, among others, have provided new insights into the dynamics, composition, and formation of asteroids and comets, contributing to a deeper understanding of the origin of the solar system. They also represent the first steps in the space exploration of small bodies, generating the possibility of a new industrial activity: space mining. This means that to bring minerals

obtained from small bodies to Earth, a spacecraft needs to travel to them. This activity will be indispensable someday, considering that the Earth has a finite amount of important minerals. In that sense, modeling the orbit of a spacecraft around irregular and small celestial bodies is one of the greatest challenges for such missions. Due to these irregular shapes, and the effect of the rotation of asteroids and comets, the gravitational fields around these bodies acting in spacecraft travelling around them are extremely complex [4]. To solve this problem, the first step in studying the orbital dynamics near these small celestial bodies is to derive mathematical models for their gravitational fields which, due to the diversity of their irregular shapes, is a task that presents major challenges. Frequently, a spherical harmonic expansion is used to model Earth and other planets, as these more massive celestial bodies (when compared to asteroids) have near spherical shapes [5]. However, when the body does not resemble a sphere, this expansion becomes inconvenient and, in some cases, convergence cannot be guaranteed [5]. Additionally, the expansion of lower-order Legendre coefficients often does not provide a good approximation for the motion of a spacecraft due to the fact that higher-order terms can lead to divergence after several iterations [6,7].

The shape of a celestial body, its rotation period, and other physical characteristics can be obtained through light curve analysis and radar analysis. From these observations, it is possible to use the polyhedral method to determine the dynamics around irregular bodies, including gravitational fields, stability, bifurcation, etc. [7–12]. However, this approach requires significant computational effort depending on the number of polyhedral shapes. The gravitational potential can be obtained with high precision using the polyhedral model. However, this model makes it challenging to analyze the effects of specific parameters, such as the system's mass ratio, the dimensions of celestial bodies, and the rotation period on spacecraft dynamics. This difficulty arises because, in the polyhedron model, the parameters produce a mixed influence on the gravitational field of irregular bodies. Therefore, to study the effect of a single parameter, it is often necessary to model irregular bodies using simplified models. By using simplified models, it is possible to perform semi-analytical studies to understand which parameters affect stability, emergence of equilibrium points, bifurcations, etc. Thus, simplified models help us to understand the dynamics around irregular bodies, and allow us to make a preliminary design of orbits [13,14], which can be refined as more information about the gravity fields becomes available and used to identify suitable landing regions. An effective way to analyze the surface of an asteroid is to hover with a spacecraft fixed in a region close to the asteroid, where the spacecraft maintains a constant position relative to the asteroid [15]. Optimal locations for using fixed-body hovering are equilibrium points, as they are locations that receive minimal disturbance. Researchers have investigated fixed-body hovering at equilibrium points and classified the varieties near these points into eight types. Fixed-body hovering can be used to obtain precise measurements of a region on the surface of the target asteroid and to facilitate the ascent and descent maneuvers of a spacecraft whose mission includes a return to Earth with samples [16].

Various bodies with different shapes can be described using simplified mathematical models. For example, refs. [5,6,17] analyzed the motion of a particle under the gravitational field of a massive straight segment. A simple flat plate [18], a homogeneous rotating cube [19], and a triaxial ellipsoid [20] were also used to model bodies with irregular shapes.

In another work [4], it was proposed that certain classes of elongated small bodies can be modeled by a double particle linkage called a dipole model. Subsequently, an investigation of dynamic properties near an elongated body (using the dipole model) was made [21] to analyze the influence of force ratio (k), mass ratio (μ), and flattening of the primary body on the distribution of equilibrium points in the x - y plane. The concept of a rotating mass dipole applied to binary asteroid systems was introduced [1]. The motion of an infinitesimal mass particle in the vicinity of a binary asteroid system was also investigated [1] considering the restricted synchronous three-body problem. The authors assumed that the most massive body in the system is treated as a point mass m_1 , while the

smaller body is modeled as a rotating dipole consisting of masses m_{21} and m_{22} , as shown in Figure 1.

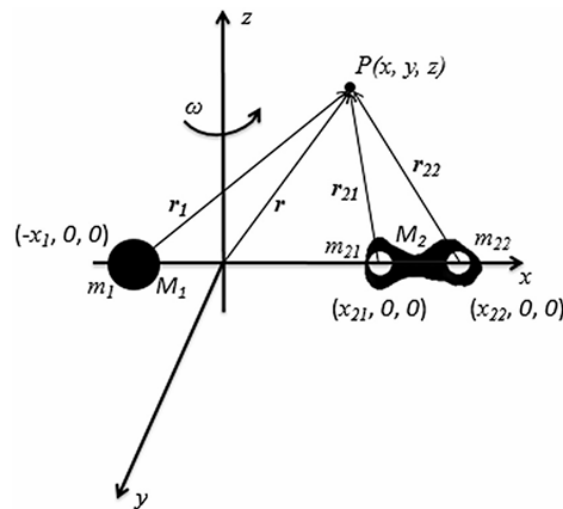


Figure 1. Representative image of the geometric shape of the system under study (not in scale) [1].

Previous studies have investigated the influence of the secondary body's dimensions and the system's mass distribution on stationary solutions, such as equilibrium points, bifurcations, planar periodic orbits, stable and unstable regions, and how these parameters affect the stability of equilibrium points [1,22]. Inspired by this research [1], several subsequent works have explored spacecraft dynamics near binary asteroid systems, modeling the primary body as a point mass (spherical body) and the secondary as a rotating mass dipole. Building on previous work [1], further studies considered scenarios where the primary and secondary bodies move in elliptical orbits around their center of mass [23]. Their investigation attempted to demonstrate the impact of the eccentricity of the orbits of the asteroids on the existence and stability of equilibrium points, which helps in understanding spacecraft motion near asteroid systems. After that, reference [24] extended the work done in [23] to examine the stability and sensitivity of equilibrium points in the restricted elliptical three-body problem considering an oblate primary and a secondary as a dipole for binary systems, with application to the systems Luhman 16 and HD188753. The influence of the body parameters on the emergence of equilibrium points and their stabilities were also investigated [24]. The restricted synchronous three-body problem was further examined, considering that the most massive body is spherical, while the less massive one is elongated and modeled as a dipole [25]. The dipole consists of two connected masses. These studies, among others, have demonstrated that simplified models makes it possible to analyze the dynamics of a satellite near irregularly shaped asteroids. It is also possible to identify the main parameters of the system that significantly influence solutions, whether stationary or not, around certain asteroid systems [1,22,25]. Specific trajectories can be studied using more precise models when considering the final stages of a real mission, but a general understanding of the gravitational field based on a small number of parameters is very useful in the early stages of mission design.

The equilibrium points that arise in the circular restricted three-body problem are of great importance for applications in the field of astronautics [26,27]. Using the circular restricted three-body model, there are five equilibrium points that emerge from the solutions of the equations of motion. This means that, if a particle is placed at one of these points with zero initial velocity relative to the rotating coordinate system, it will remain indefinitely at that point. The collinear points (L1, L2 and L3) are always unstable. On the other hand, the triangular points (L4 and L5), depending on the mass ratio, can be either unstable or linearly stable [26,27]. Whether unstable or not, all these points are ideal locations for placing a space station, because they require a small amount of ΔV (and fuel) to keep the

spacecraft around the equilibrium point. The triangular points are generally better suited for this purpose, as they are often linearly stable equilibrium points [26,27].

Sometimes it is necessary to transfer a spacecraft from one equilibrium point to another. This happens to use the spacecraft to observe a different point in space or to study the space around the system during the transfer. Previous works have analyzed orbital maneuvers between equilibrium points. Among these studies, we can highlight one that examined transfer orbits using the circular restricted three-body problem focusing on the Lagrangian points of the Earth–Moon system [28]. In this study, transfers from the Lagrangian points L1, L2, L4 and L5 to the Moon were investigated [28], as well as transfers from the Moon to these points, utilizing the mirror image theorem [29,30]. Orbital transfers within the Earth–Moon system were also investigated, with a focus on transfer orbits from the five Lagrangian points to the Earth [31]. Another interesting study in the field of transfers between Lagrangian points was conducted [32], in which the authors analyzed orbital transfers between the Earth and all the Lagrangian points of the Sun–Earth system, taking into account the perturbation of a fourth body (the Moon). An interesting application of the L1 point in transfers to the Moon is also available in the literature [33]. A more recent study [34] analyzed transfer orbits between equilibrium points around an elongated asteroid. In this study, the author examined transfer orbits around asteroid 433 Eros. Another study [35] investigated the effect of radiation pressure in a Sun–Asteroid system. In this work, it was noted that radiation pressure plays a significant role in the transfer process, particularly in systems formed by asteroids, as their gravitational forces are smaller compared to systems with larger bodies.

This study explores the dynamics of spacecraft trajectories in transfers between collinear equilibrium points in binary asteroid systems, focusing on the effects of perturbative forces such as solar radiation pressure (SRP) and the non-spherical geometry of one of the primary bodies. Using the two main components of the asteroid system 2001 SN263 (alpha-gamma) as a reference, we incorporate the elongated shape of the smaller asteroid (gamma), represented as a rotating mass dipole, into the dynamical model. Unlike conventional approaches that approximate binary asteroid bodies as point masses, this work highlights the importance of considering their irregular geometries and associated perturbations. A similar study in transfers between Lagrangian points using these dynamics is the main contribution of the present research, because it was never done in the literature.

Building on previous studies, which primarily examined gravitational effects and included SRP in simpler contexts, this research aims to analyze bi-impulsive transfers in a model that integrates both SRP and the non-spherical shape of the secondary asteroid. The study seeks to explore how these factors influence the characteristics of the transfer trajectories and the required velocity impulses, with a focus on optimizing fuel consumption for maneuvers, but also mapping general solutions that can be used for different purposes, like studying the space near the double asteroid system.

This work uses the physical and orbital characteristics of the Alpha and Gamma bodies of 2001 SN263 as a basis for simulations, providing a case study for exploring how perturbations affect transfers in binary systems. This investigation is expected to offer insights into mission planning in dynamically complex environments, contributing to the broader understanding of orbital dynamics in binary asteroid systems. Table 1 shows the physical and orbital parameters of the primary body and the secondary body analyzed.

The locations of the equilibrium points under SRP are time dependent, because the orientation of the spacecraft and its distance from the Sun influence their locations. Since this problem was studied before and the new aspect proposed for the present paper is to evaluate effects of a more complex dynamics in the transfer trajectories, we did not include SRP when determining the locations of the equilibrium point. Time dependent locations of the equilibrium points would also affect the transfer trajectories and would not allow us to study only the transfer trajectories. We also assumed that the “dipole-shaped” smaller primary is always self-aligned due to the tidal forces.

Table 1. Physical and orbital parameters of the binary asteroid system.

		Primary	Secondary
Mass	Canonical Unity	0.989432	0.010574
	International System of Units	917×10^{10} kg	9.8×10^{10} kg
Dimension	Canonical Unity	Diameter = 0.73606	Dimension (d) = 0.18664
	International System of Units	Diameter = 2800 m	Dimension (d) = 700 m
Semi-major axis	Canonical Unity		1
	International System of Units		3804 m
Orbital Period	Canonical Unity		2π
	International System of Units		59,270.4 s

2. Equations of Motion and Methodology

In this study, we will use dynamics based in the gravitational effects of the larger body, which is assumed to be a point of mass, a smaller body that is composed of two points of mass and the solar radiation pressure, which is assumed to be acting only in the infinitesimal mass, because the asteroids have masses too large to be affected by this force. So, the equations of motion for the negligible mass body, in the x – y plane, as observed from a rotating reference frame, are given by Equations (1) and (2). Since all the points involved in the transfers are coplanar, there is no need to model this problem in three dimensions. Any transfers that are out of this plane would have higher costs to leave and return to the orbital plane of the primaries, so they are not considered in the present study.

$$\ddot{x} - 2\dot{y} = -\frac{(1 - 2\mu^*)(x - x_1)}{\left((x - x_1)^2 + y^2\right)^{\frac{3}{2}}} - \frac{\mu^*(x - x_{21})}{\left((x - x_{21})^2 + y^2\right)^{\frac{3}{2}}} - \frac{\mu^*(x - x_{22})}{\left((x - x_{22})^2 + y^2\right)^{\frac{3}{2}}} + P_{rad_x} \quad (1)$$

$$\ddot{y} + 2\dot{x} = -\frac{(1 - 2\mu^*)y}{\left((x - x_1)^2 + y^2\right)^{\frac{3}{2}}} - \frac{\mu^*y}{\left((x - x_{21})^2 + y^2\right)^{\frac{3}{2}}} - \frac{\mu^*y}{\left((x - x_{22})^2 + y^2\right)^{\frac{3}{2}}} + P_{rad_y} \quad (2)$$

where $x_1 = -2\mu^*$, $x_{21} = -2\mu^* - d/2 + 1$ and $x_{22} = -2\mu^* + d/2 + 1$, and d , given in canonical units, is the distance between the mass points m_{21} and m_{22} . μ^* is defined as shown in Equation (3). Note that, if we make $d = 0$, x_{21} and x_{22} will be equal and the second and third terms can be combined in a single term that corresponds to the circular restricted three-body problem.

$$\mu^* = \frac{m_{22}}{m_1 + m_{21} + m_{22}}. \quad (3)$$

Here P_{rad_x} and P_{rad_y} represent the components x and y , respectively, of the acceleration due to solar radiation pressure, as shown in Equation (4) [36,37].

$$P_{rad} = -P_S C_r \frac{A}{m} \frac{r_0^2}{R^2} \hat{r}, \quad (4)$$

where $P_S = 4.55 \times 10^{-6}$ N/m² is the solar radiation pressure in the orbit of the Earth and C_r is the coefficient of radiation pressure. C_r is a factor that depends on the reflectivity of the spacecraft, where $C_r = 1.5$ was used in the simulations during the transfer. R is the Sun–Spacecraft distance, r_0 is the Sun–Earth distance and \hat{r} is the radial direction of the Sun relative to the spacecraft. Finally, A is the effective area of the spacecraft illuminated by the Sun and m is the mass of the spacecraft [36,37].

It is important to note that the equations of motion 1 and 2 do not correspond to the photo gravitational circular restricted three-body problem (PCR3BP). In the PCR3BP framework, the primary body emitting radiation, such as the Sun, is part of the binary system, and the effects of solar radiation pressure (SRP) are included through a reduced

mass parameter. In our study, the configuration is different. We analyze a binary asteroid system where the secondary body has an irregular shape modeled as a rotating mass dipole, while the Sun acts as an external source of perturbation. The SRP from the Sun is incorporated as additional force acting on the spacecraft. This model captures both the influence of the irregular geometry of one of the primary bodies and the perturbative effect of solar radiation pressure, which differs significantly from the assumptions in the PCR3BP.

The system of Equations (1) and (2) does not have analytical solutions, so requiring numerical integrations to solve the problem. To obtain the solutions, the problem is treated as a TPBVP (Two-Point Boundary Value Problem), and it is solved using numerical integrations combined with the gradient method [31]. The following steps are used to solve the TPBVP in this work:

- (i) An initial value for the position (\vec{r}_i) and velocity (\vec{v}_i) must be provided. In this way, the complete initial state is known. The initial position is given by the problem statement (the initial equilibrium point), and the initial velocity is a variable to be determined using an iterative method.
- (ii) Next, a final time τ must be defined, and the equations of motion are integrated from the initial to the final time.
- (iii) Finally, the final position obtained from the numerical integration is compared with the desired final position (the final equilibrium point). If there is agreement between these values (with a difference smaller than a specified error), the solution is found, and the process is stopped. If there is no agreement, an increment is applied to the initial velocity and final time, and the process returns to step (i).

The method used to find the increment in the initial guess variables is the standard gradient method, as described in [38]. The routines available in this reference were used in this work with minor modifications.

The maneuvers are assumed to be bi-impulsive, meaning that the maneuver starts with the application of the first impulse at the spacecraft's initial position, which in our case is the initial equilibrium point, and ends with the application of the second impulse at the spacecraft's final position, the final equilibrium point. Figure 2 provides a representative image of how the transfers are performed for a transfer orbit in the upper semi-plane, that we called transfer orbit 1. A transfer is also possible in the lower semi-plane, which is obtained just by inverting the senses of the impulses applied. In this transfer a Δv_1 is applied at L1 to start the transfer and a $\Delta v_1'$ is applied at L3 to complete the transfer.

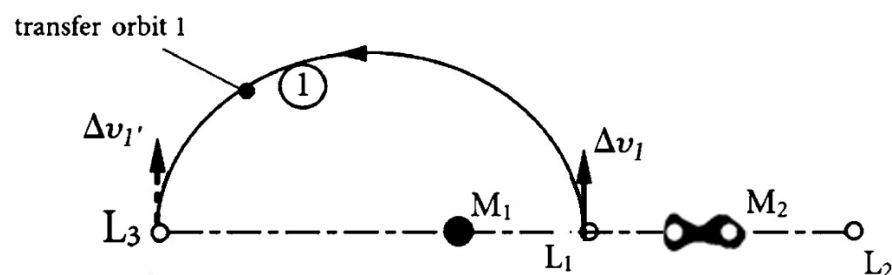


Figure 2. Transfer from the L1 Lagrange point to L3.

It is always assumed that the spacecraft is initially positioned at one equilibrium point in the binary asteroid system and aims to change its position during the mission to another equilibrium point to study and collect information about the bodies in this system from a different observational point and/or to study the space around the system during the transfer.

In the transfer from equilibrium point L1 to equilibrium point L3 that is shown in Figure 2, the orbital transfer simulations were performed for a defined range of transfer times, spanning from 0.1 days to 1.0 day. Consequently, the analysis focuses on transfer times within this range, ensuring that any solutions obtained reflect the conditions considered in this study. The simulation time range was chosen because the binary asteroid system has a

short rotation period (less than one day). Additionally, since the simulation assumes that the spacecraft is at perihelion to evaluate SRP effects, the Sun–spacecraft distance changes minimally over this time, allowing the approximation of a nearly constant solar influence. Transfer times below this range generate too large impulses and times above this range may require more refined models, in particular including the motion of the Sun. The numerical integrations were performed using the fourth-order Runge–Kutta method.

3. Results

Next, some results are presented as applications of the work developed in this study. Transfers involving equilibrium points in the 2001SN263 are used for these simulations.

3.1. Equilibrium Points

Prior to simulating the orbital transfers, we calculated the equilibrium points of the system under investigation. The equilibrium points of the binary asteroid system were determined by considering only gravitational effects of the primary bodies. This approach extends the classical restricted three-body problem (CR3BP) by incorporating the non-spherical nature of the smaller primary body, allowing for a more accurate representation of the equilibrium points in the vicinity of these bodies. The positions of these equilibrium points are determined disregarding solar radiation pressure by setting the last term of the right-hand side of Equations (1) and (2) to zero. The reason for excluding the SRP in the determination of the equilibrium points is that those points would be time dependent, if SRP is included, because the location of the Sun changes with time, as well as the attitude of the spacecraft, and those two factors change the locations of the equilibrium points. Remember that the new aspect of the proposed research is to evaluate the effects of more complex dynamics in the transfer trajectories, including transfer time and cost, so we need to remove variations in the locations of the equilibrium points from the problem. SRP is included only during the analysis of the spacecraft's transfer trajectories between equilibrium points. This allowed us to study its impact on the transfer paths while keeping the equilibrium points fixed. To mitigate the influence of SRP on a spacecraft positioned at an equilibrium point, it is possible to assume that the spacecraft's solar panels are oriented such that they are parallel to the solar rays, resulting in an effective area of zero for the SRP interaction, or that they are not deployed before starting the transfer and after finishing it. These assumptions effectively nullify the SRP at the equilibrium points.

By numerically solving this system of equations, the locations of the equilibrium points can be identified. In this study, we consider that $\mu^* = 0.005284$ and that the size of the asteroid, modeled as a rotating mass dipole, is $d = 0.186645$ canonical units [1]. These values are based on the binary asteroid system formed by the bodies alpha and gamma of the asteroid system 2001SN263. Remember that it is not our intention to study this system in detail; we just want to use data from a real system for the simulations, so we neglected the body beta, which is far from the two central ones. Gamma, one of the bodies in this asteroid system, is elongated and exhibits synchronous rotation [39]. This choice is motivated by the fact that a mission to this asteroid system is currently under consideration. Additionally, we assume that the distance between the most massive asteroid (M1) and the center of mass of the elongated asteroid (M2) is equal to 1, a consequence of using a canonical unit system.

By numerically solving Equations (1) and (2), we calculated the locations of the equilibrium points, considering the system modeled as point masses ($d = 0$) and also taking into account the irregular shape of the secondary body, which is represented as a dipole ($d = 0.186645$). In each scenario, five real roots were found. These equilibrium points serve as the foundation for initiating the orbital transfers. It was necessary to estimate the positions of the equilibrium points in both models (point mass and dipole) in order to execute the transfers from the correct stationary points. Three of these roots are located along the x -axis and are referred to as collinear solutions. The remaining two solutions lie in

the x - y plane and are known as non-collinear solutions. The positions of these equilibrium points in the two adopted models are illustrated in Tables 2 and 3.

Table 2. Positions of the equilibrium points considering the point mass model.

	x_0	y_0
L1	0.844975	0
L2	1.149281	0
L3	−1.00440	0
L4	0.48942	0.86602
L5	0.48942	−0.86602

Table 3. Positions of the equilibrium points considering the dipole model.

	x_0	y_0
L1	0.803777	0
L2	1.191579	0
L3	−1.00441	0
L4	0.49279	0.86412
L5	0.49279	−0.86412

3.2. Orbital Transfers

Orbital transfer simulations were conducted between the Lagrange points L1 and L2, as well as between L1 and L3 in the asteroid system. These simulations obtained five key parameters: the transfer time, the required velocity change (ΔV) for each maneuver, the initial flight path angle (fpa), and the spacecraft's positions x and y throughout the trajectory. The angle fpa is defined such that it is zero on the x -axis pointing in the positive direction, increasing counterclockwise, as illustrated in Figure 3. This angle represents the initial fpa direction of the spacecraft, a critical parameter for determining the trajectory.

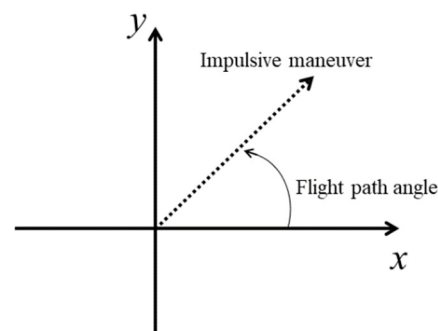


Figure 3. Flight path angle (fpa).

The first family of transfer orbits considers transfers between the collinear equilibrium points L1 and L2, assuming that the asteroid is at perihelion in its orbit around the Sun, approximately 1.03617286 A.U. (A.U. = Astronomical Unit, which is the average Sun–Earth distance). The second family of transfer orbits focuses on transfers between the collinear Lagrange points L1 and L3, also assuming that the asteroid is at perihelion. Plots of transfer time versus ΔV , fpa versus ΔV , and the transfer orbit trajectories are presented in a rotating reference frame. The position of the asteroid in its orbit around the Sun is very important because the Sun–Asteroid distance significantly affects the solar radiation pressure.

In the orbital transfer simulations, we used a reflectivity coefficient (C_r) of 1.5 for the spacecraft. The solar radiation pressure (P_S) is assumed to be 4.551×10^{-6} N/m², and the

area-to-mass ratio (A/m) is $0.01 \text{ m}^2/\text{kg}$. The red curve (red circle) represents the situation where the primary is a point mass and the secondary is a rotating mass dipole, while the green curves (green squares) show the results obtained using point of mass model for both asteroids.

Figure 4 illustrates how the transfer time correlates with the required ΔV for orbital maneuvers between $L1$ and $L2$ equilibrium points. The left side of Figure 4 shows the ΔV as a function of transfer time for the entire range of transfer durations (0.1 until 1 day). The right side of Figure 4 is a zoom-in on a specific region of the left side, highlighting the areas with the minimum ΔV required for the transfers from the $L1$ equilibrium point to $L2$. Observe in the figure (right side) that solutions with minimum ΔV for performing the transfer between the analyzed points are highlighted with black and purple circles, corresponding to the dipole model and point mass model, respectively. The analysis shows that, for shorter transfer times, approximately less than 0.7 days, the ΔV needed for the maneuver is similar for both models: the classic Circular Restricted Three-Body Problem (CRTBP), which is the model used when the two asteroids are assumed to be points of mass, and the dipole-extended model. The initial flight path angle (fpa) also exhibits minimal differences under these conditions. However, when the transfer time exceeds 0.7, the disparity between the models becomes more pronounced. Solutions that are feasible within the mass points model are no longer achievable when the dipole model is applied, highlighting the differences introduced by the elongated shape of the less massive primary. This is a consequence of the fact that for longer transfers more time is available for the perturbations to act in the system and the differences are very important.

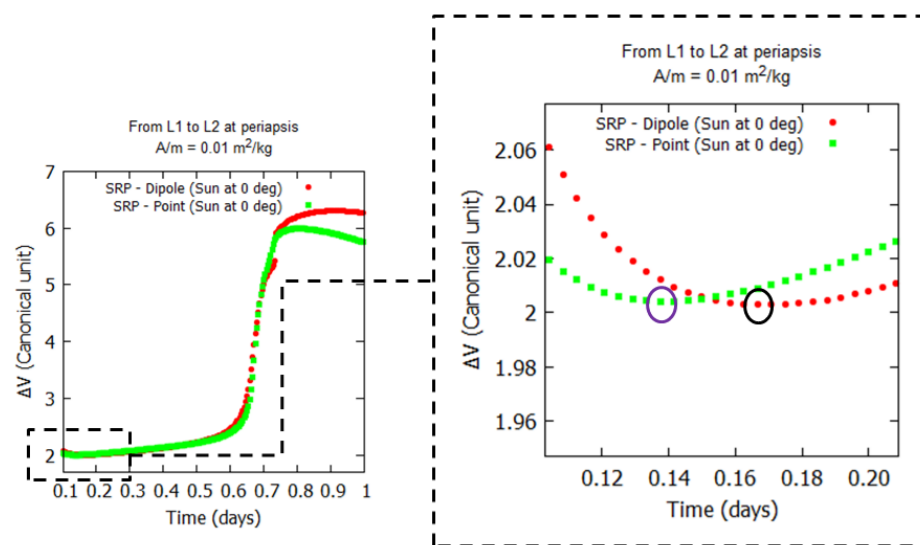


Figure 4. Transfers from $L1$ to $L2$. The green curve (squares) represents the case where the bodies are modeled as point masses. The red curve (circles) represents the situation where the secondary is a rotating mass dipole.

Figure 5 can be interpreted in the same way as Figure 4, with the difference that it shows ΔV as a function of the fpa . The left side of Figure 5 displays the complete simulation, while the right side is an approximation of a region with the minimum ΔV required to perform the transfer. For shorter transfer times, the required fpa remain similar for the two models, reinforcing the similarity of the dynamics in this regime. As the transfer time increases, however, the impact of the elongated primary becomes evident, with the dipole model imposing distinct conditions on the fpa compared to the CRTBP. This divergence illustrates the limitations of point mass models in capturing the full complexity of systems involving non-spherical bodies. Together, these findings provide a comprehensive evaluation of the transfer dynamics, demonstrating how transfer time, fuel consumption (ΔV), and initial impulse direction (fpa) are interconnected. The comparative

analysis of the CRTBP and dipole model emphasizes the significance of considering the actual shapes of the bodies involved. Notably, the elongated configuration of the secondary has a substantial effect on fuel consumption and the feasibility of certain maneuvers, particularly at longer transfer times. These insights enhance our understanding of how realistic modeling can impact the planning and execution of orbital maneuvers.

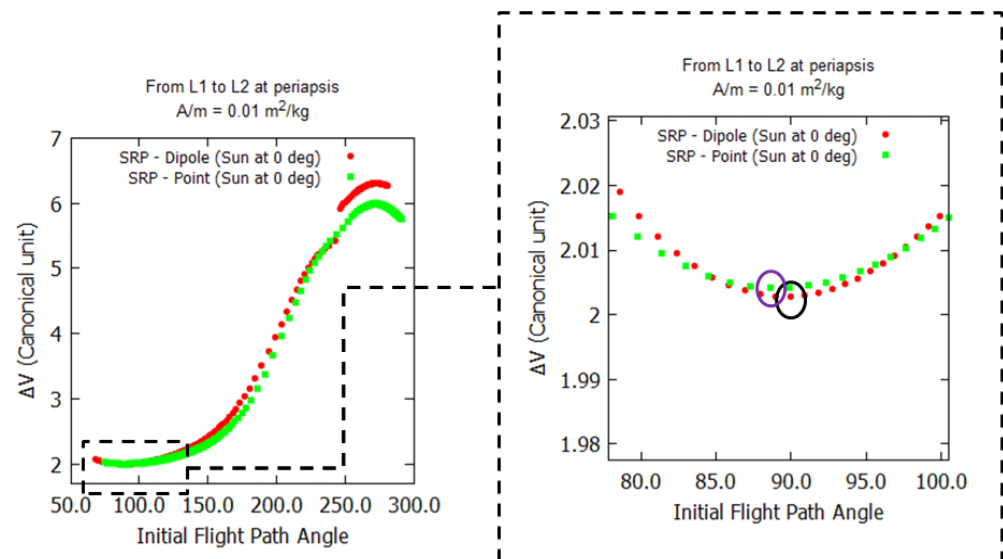


Figure 5. Transfers from L1 to L2. The green curve represents the case where the primary bodies are modeled as point masses. The red curve represents the situation where the more massive body is a point mass and the less massive primary is a rotating mass dipole.

Figures 4 and 5 are related in the sense that they both represent the ΔV required for the transfers from L1 to L2. While Figure 4 shows the relationship between transfer time and ΔV , Figure 5 shows the variation of ΔV with the initial flight path angle (fpa). Both plots are based in the same simulations, they just show different relations. Figure 4 shows how the variation of velocity is related to the time of flight, while Figure 5 gives the direction to apply the impulse and the magnitude of the impulse. So, the complete information is available and we know how to apply the impulse.

The results shown in Figure 5 indicate a strong dependence of the effects of the shape of one of the asteroids with transfer time. For longer transfer times the effects are larger, as expected, since the perturbations caused by the elongated shape have more time to affect the trajectory. It is clear that, after about 0.7 days of transfer time, the more accurate model considering the shape of one of the asteroids requires larger variations of velocity, so it is necessary to use more fuel to compensate the extra force given by the irregular shape of the asteroid. For faster transfers, there is not enough time for the perturbation to give important results in terms of fuel consumption, so the two lines are near each other.

Figure 6 was constructed to provide a different view of the interactions between transfer time, flight path angle (fpa), and ΔV , demonstrating that these parameters are interconnected. In Figure 6, the parameters determining the minimum ΔV required for the transfer in the dipole model are shown. It is also noticeable that, as the transfer time increases, the fpa becomes larger, resulting in a higher ΔV needed to perform the transfer.

Figure 7 illustrates specific spacecraft trajectories during the transfer from point L1 to point L2. This figure displays both the minimum and maximum ΔV trajectories for both models. The black and red trajectories represent the minimum ΔV solutions for the dipole model and point mass model, respectively, corresponding to the solutions highlighted with black and purple circles on the right side of Figures 4 and 5. The blue (dipole model) and pink (point mass model) trajectories indicate the transfers requiring the highest ΔV .

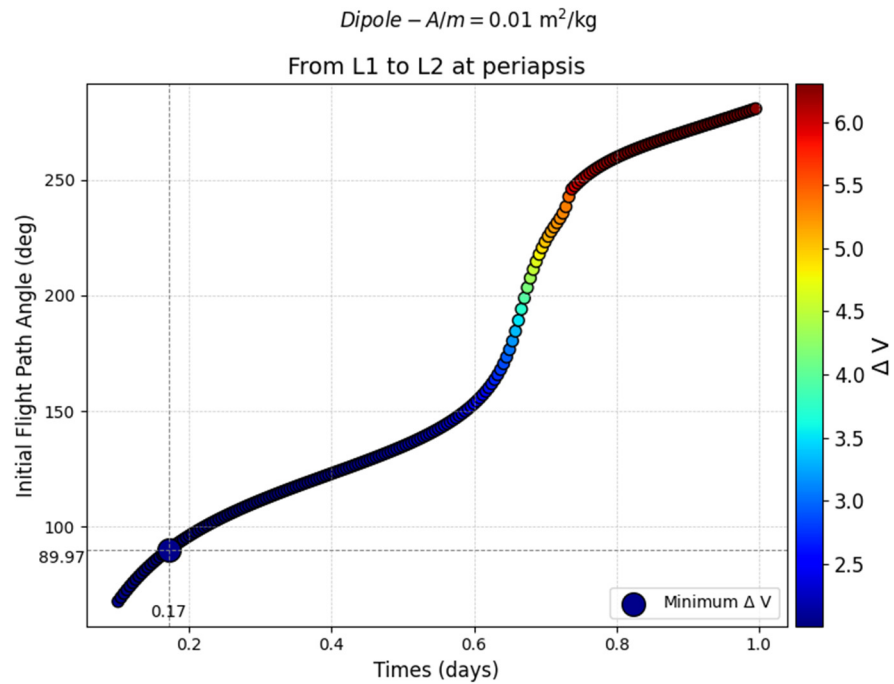


Figure 6. Illustration of the interactions between transfer time, flight path angle (*fpa*), and ΔV from L1 to L2.

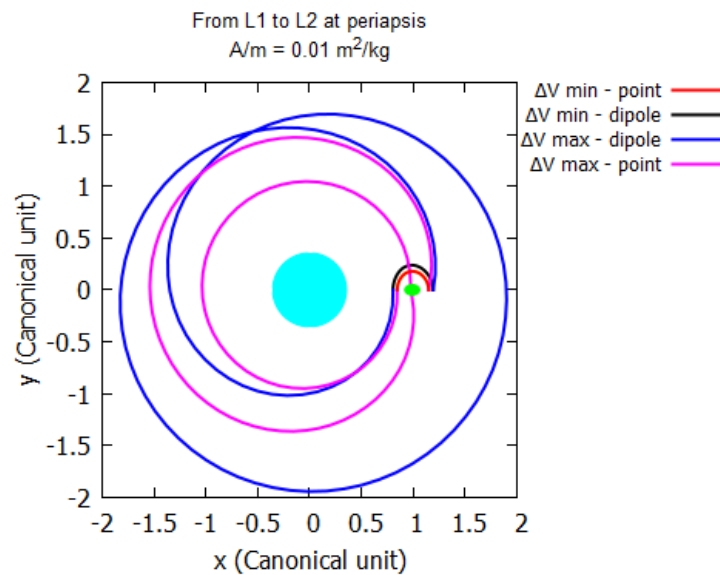


Figure 7. Transfers of a spacecraft from point L1 to point L2. Trajectories illustrating transfers with minimum and maximum ΔV . Red and black represent the minimum ΔV for point mass and elongated secondary models, respectively, while pink and blue indicate the maximum ΔV for these models.

It is important to note in Figure 7 that the transfer requiring the maximum ΔV (represented by the pink trajectory) initially intersects with the secondary body. However, when the dimensions of the secondary body are taken into account, the trajectory is naturally influenced by the system’s dynamics, preventing a collision. This difference underscores the importance of considering the body’s size in mission planning to ensure a safe and viable transfer.

The analysis of Figure 8 is similar to that of Figure 4, but it illustrates how the ΔV required for the transfer from the L1 equilibrium point to L3 varies with flight time. In Figure 8, it can be observed that the solutions are similar whether we consider the point mass model for both bodies (green squares) or the dipole mass model (red circles). Unlike

the transfers from L1 to L2, the L3 point is located far from the secondary body, meaning that the spacecraft's trajectory is significantly influenced by the secondary body's size for a short part of the transfer. As the spacecraft moves toward L3, its distance from body M2 increases, causing the elongated shape of the secondary to have a reduced effect on the spacecraft's path. It is noteworthy from Tables 2 and 3 that the location of L3 remains almost the same, showing that it is not significantly affected by the elongated shape of M2. In Figure 8, a dashed black rectangle highlights a specific region containing transfer solutions that result in collisions with the primary body. These trajectories, while feasible in terms of ΔV and flight time, are ultimately unviable for the transfer due to their intersection with the primary, but they can be used for end-of-life maneuvers. In many missions, a collision with a celestial body is made in the end of the mission, since it allows the possibility of further studies in the system. These results emphasize the need for careful consideration of collision constraints in transfer planning, even when ΔV optimizations are prioritized.

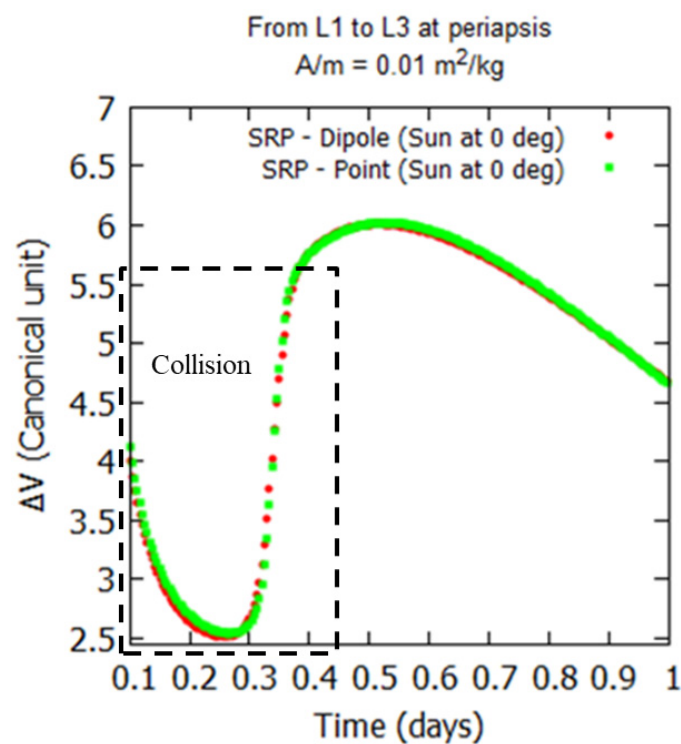


Figure 8. Transfers from L1 to L3. The green curve (squares) represents the case where the primary and secondary bodies are considered as point masses. The red curve (circles) represents the scenario where the primary is modeled as a point mass, and the secondary is modeled as a rotating mass dipole.

Figure 9, similar to Figure 5, explores the impact of the initial fpa on ΔV requirements for the transfer from L1 to L3. In this figure, the green curve again represents the scenario where the primary bodies are modeled as point masses, while the red curve shows the scenario where the less massive primary is modeled as a rotating mass dipole.

Figure 9 illustrates that the shapes of the curves (green and red) are similar, however, the initial fpa required for the spacecraft to depart from L1 and reach L3 differs due to the non-spherical nature of the secondary body. When the elongated shape of the secondary is taken into account, the initial fpa must be less than 180 degrees for the spacecraft to achieve a transfer to L3 with minimal ΔV . In contrast, when the secondary body is modeled as a point mass, the initial fpa must exceed 180 degrees to reach L3 with minimal ΔV . This highlights the critical importance of considering the elongated shape of the secondary body in mission planning, as it significantly impacts the trajectory and the ΔV requirements for a successful transfer.

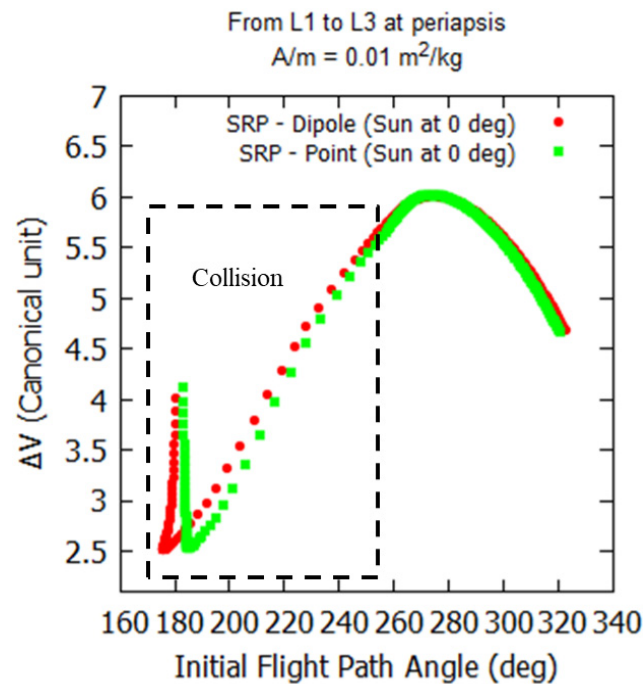


Figure 9. Transfers from L1 to L3. The green curve (squares) represents the case where the bodies are modeled as point masses. The red curve (circles) represents the situation where the more massive body is a point mass and the secondary is a rotating mass dipole.

A dashed black rectangle highlights regions where transfer solutions result in collisions with the secondary body. Although the primary focus of this study is on successful transfers, these collision solutions are worth noting. As already mentioned, such trajectories, achievable with minimal ΔV , could be of particular interest for missions targeting controlled impacts with an asteroid, such as planetary defense tests or resource utilization endeavors. This observation underscores the versatility of the methodology presented, demonstrating that lower impulse solutions can efficiently guide a spacecraft to either avoid or deliberately collide with a target body, depending on the mission's objectives.

Following the approach used in Figure 6, Figure 10 was constructed to illustrate the relations between the parameters analyzed for a transfer from L1 to L3. The x-axis represents the transfer time, the y-axis indicates the fpa , and the color coding corresponds to the ΔV required to complete the transfer. Figure 10 highlights that the transfer time required to minimize ΔV (without collision) is 1.0 days, with an fpa of 322.53 degrees, when the dipole model is considered.

Figure 11 illustrates specific spacecraft trajectories during the transfer from L1 to L3. This figure shows both the minimum and maximum ΔV trajectories for both models. The black and yellow trajectories (superimposed trajectories) represent the minimum ΔV solutions for the dipole model and point mass model. The blue (dipole model) and pink (point mass model) trajectories indicate the transfers requiring the maximum ΔV . Finally, the red trajectory represents the minimum ΔV when there is no collision with the bodies in the system.

It is important to note, in Figure 11, that the transfer requiring the maximum ΔV (represented by the pink trajectory) will eventually collide with the secondary body.

However, when the dimensions of the secondary body are taken into account, the trajectory is naturally altered (blue trajectory) by the system's dynamics, preventing a collision. This difference underscores the importance of considering the body's size in mission planning to ensure a safe and viable transfer.

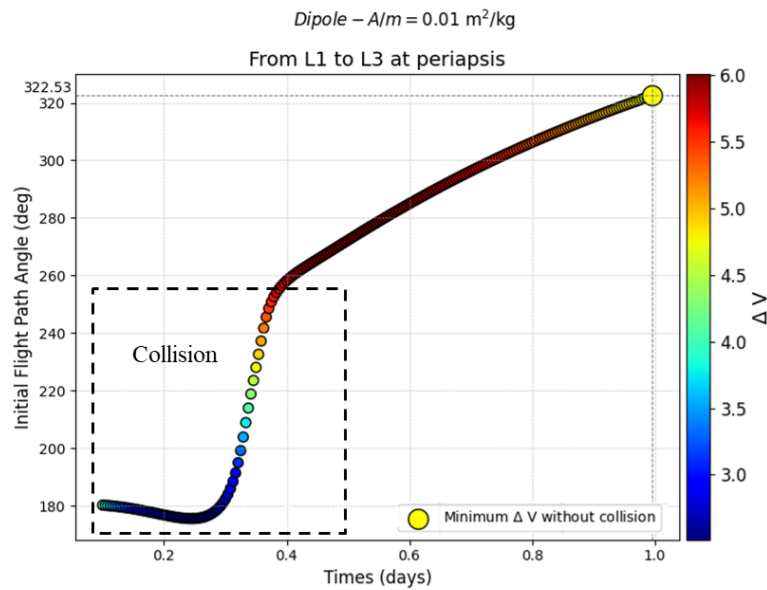


Figure 10. Illustration of the relations between transfer time, flight path angle (*fpa*), and ΔV from L1 to L3.

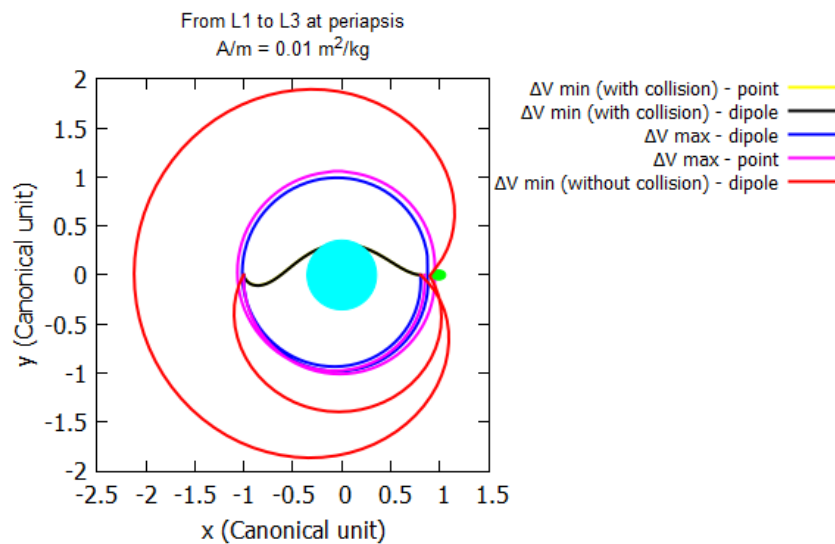


Figure 11. Transfers of a spacecraft from L1 to L3. The yellow and black (superimposed trajectories) orbits represent the minimum ΔV , point of mass and dipole model, respectively. The pink and blue orbits represent the maximum ΔV , point of mass and dipole model, respectively. The red trajectory represents the minimum ΔV without collision, considering the dipole model.

This highlights the critical impact of including the geometric and dynamical complexities of the system, as longer transfer times under the realistic model not only increase the ΔV requirements but also introduce potential collision risks that are absent in the point-mass approximation.

After analyzing the results with the asteroid always positioned at periapsis, we decided to perform an analysis varying the Sun’s angular position to observe any changes in the orbital transfer results. From this point on, all results account for the shape of the smaller body. So, here, body M1 is considered a spherical body, and body M2 is modeled as an elongated body represented in the equations of motion as a rotating mass dipole. Figure 12 presents a graph relating ΔV to the time required for a transfer. From Figure 12, we can see that the angular position of the Sun does not significantly affect the spacecraft transfer from L1 equilibrium point to L3 point. This is due to the fact that the area-to-mass ratio used in this study is very low ($A/m = 0.01 \text{ m}^2/\text{kg}$) and the main effect of changing the location of

the asteroid in its orbit is the fact that the Sun–asteroid distance has a strong effect in the magnitude of the solar radiation force.

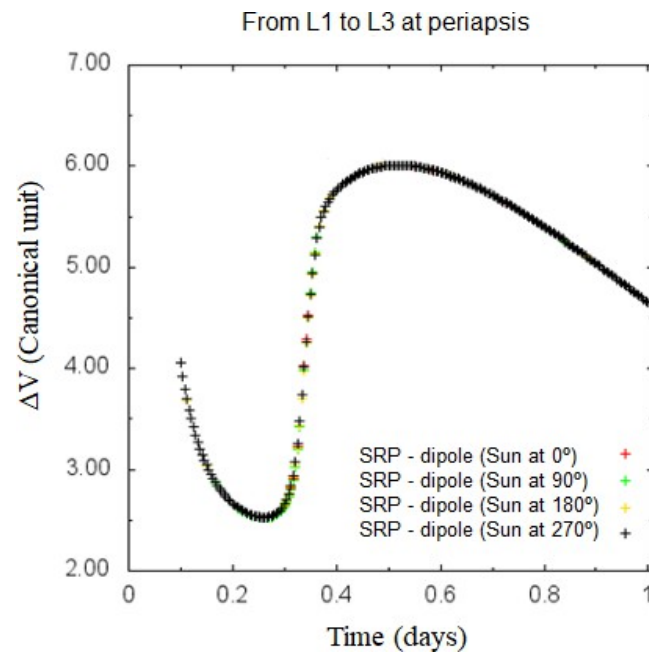


Figure 12. Transfer time versus ΔV for different positions of the Sun.

We also constructed a graph relating ΔV to the initial fpa , as shown in Figure 13. It confirms that the angular position of the Sun does not significantly change the required fpa for the transfer for the same reasons explained earlier. Since we observed that solar radiation pressure is not significant in transfers when considering a very small area-to-mass ratio, and this is a parameter that we decided to investigate in its effects in the trajectories, we increased the area-to-mass ratio. To do this, we fixed the asteroid at periapsis and varied the area-to-mass ratio. Figure 14 shows the relationship between ΔV and transfer times when performing the transfers from L1 to L3. Figure 15 shows the relationship between ΔV and the fpa when performing the transfers from L1 to L3.

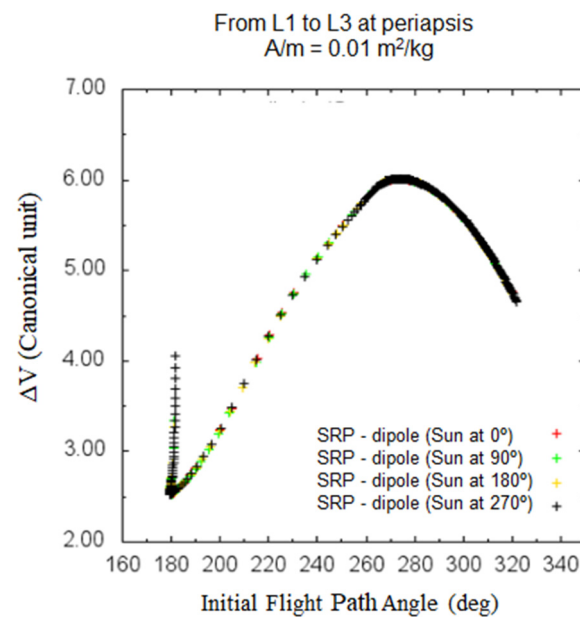


Figure 13. fpa as a function of ΔV for different positions of the Sun.

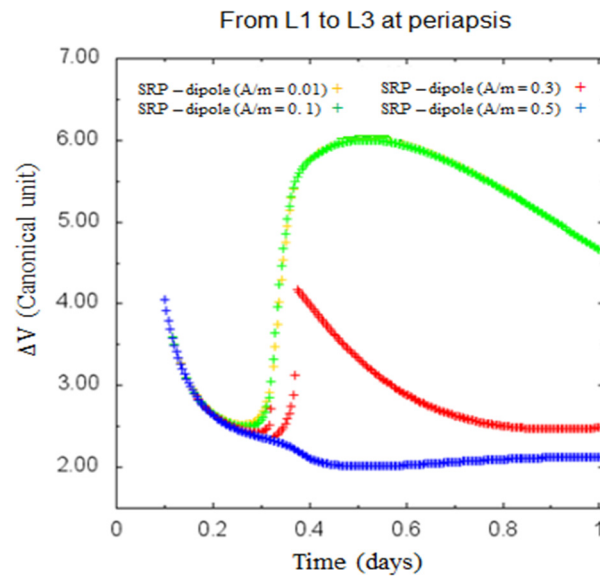


Figure 14. Transfer times versus ΔV for different area-to-mass ratios.

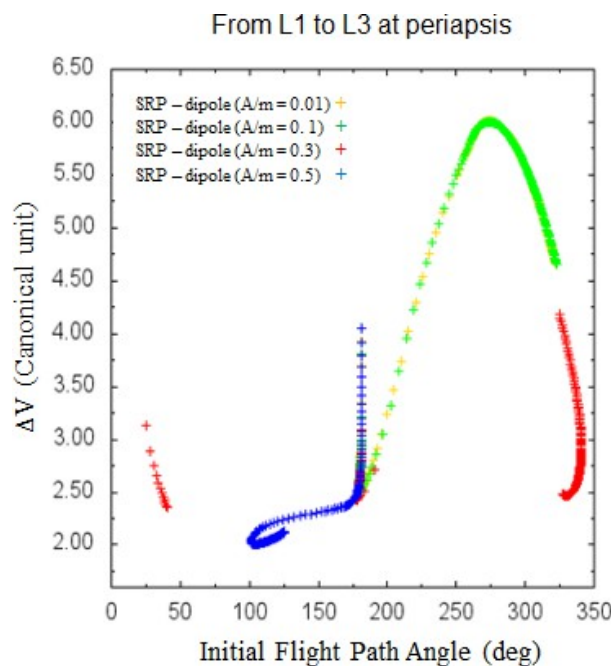


Figure 15. Initial Flight Path Angle versus ΔV for different area-to-mass ratios.

We can observe that, in Figures 14 and 15, as we vary the area-to-mass ratio, the influence of solar radiation pressure on the transfers becomes significant. We see that when $A/m = 0.5 \text{ m}^2/\text{kg}$, the ΔV required for the transfer is somewhat lower than in the other cases. To have a better understanding of the trajectories involved, Figure 16 shows the optimal transfers from L1 to L3 and their respective mass ratios.

In Figure 16, we can observe that, for $A/m = 0.01 \text{ m}^2/\text{kg}$ and $A/m = 0.1 \text{ m}^2/\text{kg}$, the spacecraft would not complete the transfer, as the satellite collides with the primary body (yellow and green trajectories, respectively). In Figure 14, the trajectories corresponding to $A/m = 0.01 \text{ m}^2/\text{kg}$ (yellow) and $A/m = 0.1 \text{ m}^2/\text{kg}$ (green) are superimposed due to their similarity. However, when the area-to-mass ratio is $A/m = 0.3 \text{ m}^2/\text{kg}$ (red trajectory), the transfer is successful. This is a risky trajectory for a space mission, because it passes very close to the surface of M1. The trajectory that requires the minimum ΔV (as shown

in Figures 14 and 15) is represented in blue in Figure 16. It can be seen that this trajectory passes at a higher altitude over body M1, making it a safer maneuver for a space mission.

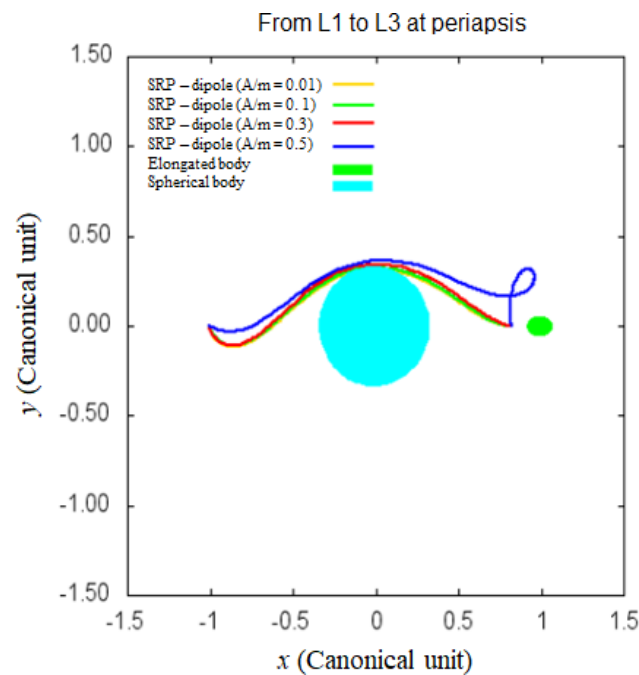


Figure 16. Trajectories from L1 to L3 considering different values for the area-to-mass ratio.

A summary of the results presented in Figures 12–16 is that solar radiation pressure has important effects when the area-to-mass ratio is above $0.1 \text{ m}^2/\text{kg}$. After this value, and for transfer times longer than 0.3 days, the solar radiation pressure becomes an important force in the dynamical model and much attention has to be given to the transfers.

It is also noted that the effect of adding the non-spherical shape of the smaller asteroid is to have a shift between clockwise and counterclockwise transfers due to the extra force, and it can cause collisions in some transfers. In this type of transfer, there is more than one solution for the TPBVP. This problem is similar to the Lambert's Problem [40], which has two solutions with less than one revolution: a clockwise and counterclockwise solution. If we allow multiple revolutions for the transfer orbit, we get two more solutions for each complete revolution allowed for the transfer. To avoid very much longer transfers we restricted the number of revolutions to less than one, so only two solutions are possible. From those two, we selected the one with minimum impulse required. As a consequence, longer transfers (above 0.3 days) have completely different dynamics. Figure 14 shows that solar radiation pressure can be used to decrease the magnitude of the impulse required for the transfers, as there are solutions with longer transfer times (from 0.3 to 1 day) that require smaller variations of velocity for larger values of the area-to-mass ratio. The trajectories shown in Figure 15 explain this in detail.

Next, we performed the same analysis for the transfers from L1 equilibrium point to L2. Figure 17 shows the ΔV required for a transfer from L1 to L2 and its corresponding fpa .

We can observe that, initially, the curves are quite similar. However, for the transfers when the area-to-mass ratio is $A/m = 0.5 \text{ m}^2/\text{kg}$, the ΔV required to perform the maneuver is slightly lower. The relationship between ΔV and the time required to complete the maneuver is shown in Figure 18.

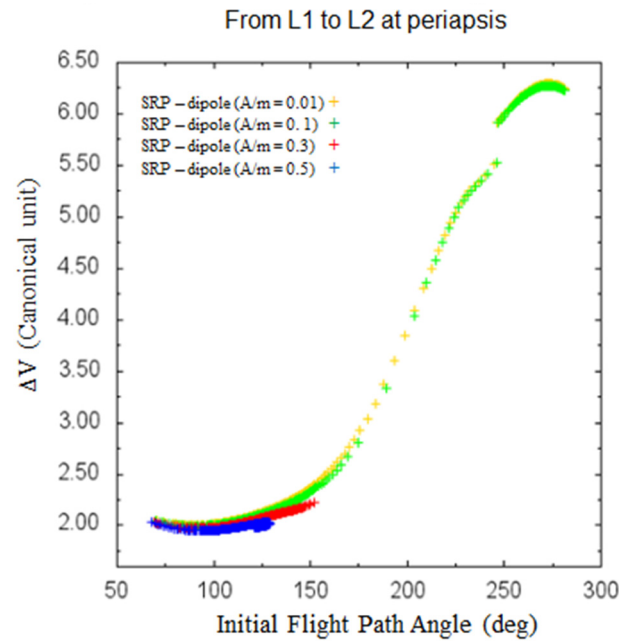


Figure 17. Transfers from L1 to L2 considering different values for the area-to-mass ratio.

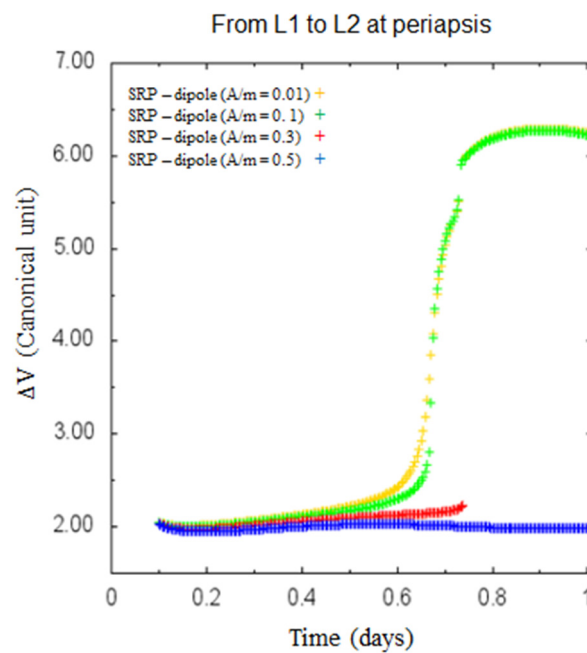


Figure 18. Transfers from L1 to L2 considering different values for the area-to-mass ratio.

Figure 19 shows the optimal transfer trajectories. Unlike that which is shown in Figure 16, none of the transfers shown in Figure 19 collide with any of the bodies.

A summary of the results of transfers from L1 to L2 showed in Figures 17–19 shows the same effect noted in transfers from L1 to L3, but with much smaller magnitudes. It means that small values for the area-to-mass ratio do not have a significant impact in the transfers, but larger values can reduce the magnitude of the impulses with the inclusion of the solar radiation pressure in the dynamical model. The reason for the reduction of the effects is that L1 and L2 are closer to each other, so the transfers have smaller length and do not pass close to M1 to generate collisions with this larger body.

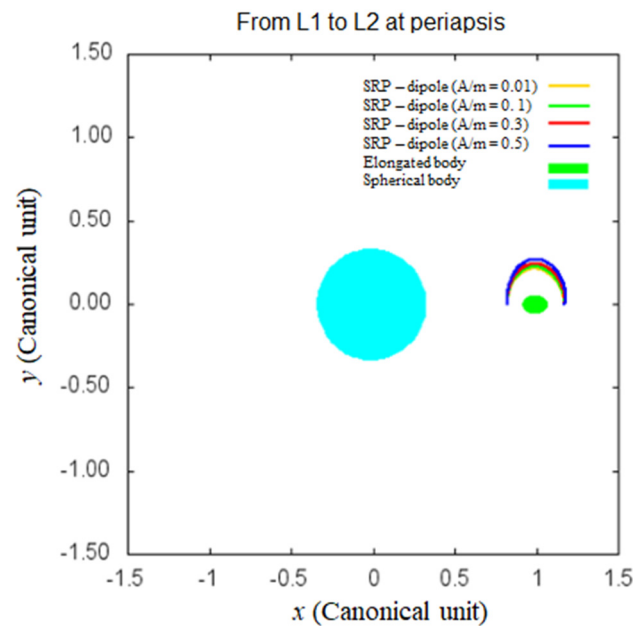


Figure 19. Trajectories from L1 to L2 considering different values for the area-to-mass ratio.

4. Conclusions

The main goal of this paper was to study spacecraft transfers between the collinear equilibrium points in a double asteroid system, particularly to evaluate the differences when adding solar radiation pressure and the non-spherical shape of the smaller asteroid of the system.

This work provided a significant advancement over existing research by integrating a rotating mass dipole model to represent the non-spherical shape of the smaller asteroid and by considering the perturbative effect of solar radiation pressure (SRP) on the transfer trajectories, which is a model that was not used in this problem before. Unlike previous studies that often approximate the system with point-mass bodies and neglect SRP, our approach delivers a more realistic and comprehensive understanding of the dynamics involved. The results presented here show that these factors can substantially change the impulse requirements for orbital transfers, leading to insights that are essential for mission planning in asteroid systems where such perturbations cannot be ignored.

The results showed that the shape of the smaller asteroid has a strong influence in the magnitude of the impulse required for the transfers between L1 and L2, in particular for longer transfer times (above 0.7 days), since the perturbations have more time to affect the trajectory.

The analysis of orbital transfers between equilibrium points L1, L2 and L3 has revealed key insights into the dynamics and the impact of modeling assumptions. When comparing the point mass and dipole models for the secondary body, we observed that the shape and physical properties of the secondary body significantly influence the transfer parameters, including the flight path angle (fpa) and the required ΔV .

For transfers between L1 and L2, the proximity of the secondary body to the equilibrium points makes its elongated shape critical in determining both the trajectories and the ΔV minima. The dipole model produces trajectories and optimal flight path angles that differ markedly from those derived under the point mass approximation. Ignoring the non-spherical nature of the secondary body could result in suboptimal mission planning, higher fuel consumption, or even trajectory failures.

In contrast, for transfers to the more distant L3, the spacecraft is less influenced by the secondary body's shape. Consequently, the solutions for the two models exhibit greater similarity, with minimal variation in ΔV and trajectory characteristics. This is

attributed to the reduced gravitational perturbations as the spacecraft moves farther from the elongated secondary.

Next, a study considering different values for the area-to-mass ratio showed that important effects occur when the area-to-mass ratio is above $0.1 \text{ m}^2/\text{kg}$, when the transfer times are above 0.3 days. Under these conditions, the solar radiation pressure becomes an important force and shifting between clockwise and counterclockwise transfers occur. This study also showed that the solar radiation pressure may be used to decrease the magnitude of the impulse required for the transfers, because there are solutions with transfer times from 0.3 to 1 day that require smaller variations of velocity for larger values of the area-to-mass ratio. The same happens for transfers from L1 to L2, but with much smaller magnitudes. The reason for these reductions is that L1 and L2 are closer to each other, so the transfers have smaller length and do not pass close to M1 to generate collisions with this larger body, avoiding the shifting between clockwise and counterclockwise transfers.

So, in general, this paper presents some new results regarding transfers between the collinear equilibrium points around a double asteroid system, in particular in analyzing the importance of more accurate models that include solar radiation pressure and a non-spherical shape for the smaller asteroid of the system.

This general conclusion showing the importance of the more accurate mathematical model when studying transfer orbits is valid for systems composed by elongated bodies, such as asteroids. It does not apply to near spherical systems like Earth–Moon and Sun–Earth systems.

Author Contributions: Conceptualization, A.F.B.A.P.; Methodology, L.B.T.S.; Software, V.M.G.; Investigation, V.Y.R. All authors have read and agreed to the published version of the manuscript.

Funding: This paper has been supported by the Ministry of Science and Higher Education of the Russian Federation under Agreement No. FSSF-2024-0005.

Data Availability Statement: The original contributions presented in the study are included in the article, further inquiries can be directed to the corresponding authors.

Conflicts of Interest: The authors declare no conflict of interest.

References

1. Barbosa Torres dos Santos, L.; Bertachini de Almeida Prado, A.F.; Merguizo Sanchez, D. Equilibrium points in the restricted synchronous three-body problem using a mass dipole model. *Astrophys. Space Sci.* **2017**, *362*, 61. [[CrossRef](#)]
2. Woo, P.; Misra, A.K.; Keshmiri, M. On the planar motion in the full two-body problem with inertial symmetry. *Celest. Mech. Dyn. Astron.* **2013**, *117*, 263–277. [[CrossRef](#)]
3. Braga-Ribas, F.; Sicardy, B.; Ortiz, J.L.; Snodgrass, C.; Roques, F.; Vieira-Martins, R.; Camargo, J.I.; Assafin, M.; Duffard, R.; Jehin, E.; et al. A ring system detected around the Centaur (10199) Chariklo. *Nature* **2014**, *508*, 72–75. [[CrossRef](#)] [[PubMed](#)]
4. Zeng, X.; Jiang, F.; Li, J.; Baoyin, H. Study on the connection between the rotating mass dipole and natural elongated bodies. *Astrophys. Space Sci.* **2015**, *356*, 29–42. [[CrossRef](#)]
5. Elipe, A.; Lara, M. A Simple Model for the Chaotic Motion Around (433) Eros. *J. Astronaut. Sci.* **2003**, *51*, 391–404. [[CrossRef](#)]
6. Riaguas, A.; Elipe, A.; Lara, M. Periodic Orbits around a Massive Straight Segment. In *Impact of Modern Dynamics in Astronomy*; Henrard, J., Ferraz-Mello, S., Eds.; Springer: Berlin/Heidelberg, Germany, 1999; p. 169.
7. Jiang, Y.; Baoyin, H. Parameters and bifurcations of equilibrium points in the gravitational potential of irregular-shaped bodies subjected to a varying external shape. *Adv. Space Res.* **2018**, *62*, 3199–3213. [[CrossRef](#)]
8. Werner, R.A. The Gravitational Potential of a Homogeneous Polyhedron or Don't Cut Corners. *Celest. Mech. Dyn. Astron.* **1994**, *59*, 253–278. [[CrossRef](#)]
9. Scheeres, D.J.; Ostro, S.J.; Hudson, R.S.; Werner, R.A. Orbits Close to Asteroid 4769 Castalia. *Icarus* **1996**, *121*, 67–87. [[CrossRef](#)]
10. Chanut, T.G.G.; Aljbaae, S.; Carruba, V. Mascon gravitation model using a shaped polyhedral source. *Mon. Not. R. Astron. Soc.* **2015**, *450*, 3742–3749. [[CrossRef](#)]
11. Yu, Y.; Baoyin, H. Generating families of 3D periodic orbits about asteroids. *Mon. Not. R. Astron. Soc.* **2012**, *427*, 872–881. [[CrossRef](#)]
12. Tsoulis, D.; Petrovic, S. On the singularities of the gravity field of a homogeneous polyhedral body. *Geophysics* **2001**, *66*, 535. [[CrossRef](#)]
13. Wang, W.; Yang, H.; Zhang, W.; Ma, G. Capture orbits around asteroids by hitting zero-velocity curves. *Astrophys. Space Sci.* **2017**, *362*, 229. [[CrossRef](#)]

14. Zeng, X.; Liu, X. Searching for Time Optimal Periodic Orbits Near Irregularly Shaped Asteroids by Using an Indirect Method. *IEEE Trans. Aerosp. Electron. Syst.* **2017**, *53*, 1221–1229. [[CrossRef](#)]
15. Wen, T.; Zeng, X. Natural landing dynamics near the secondary in single-tidal-locked binary asteroids. *Adv. Space Res.* **2022**, *69*, 2223–2239. [[CrossRef](#)]
16. Broschart, S.B.; Scheeres, D.J. Control of Hovering Spacecraft Near Small Bodies: Application to Asteroid 25143 Itokawa. *J. Guid. Control Dyn.* **2005**, *28*, 343–354. [[CrossRef](#)]
17. Riaguas, A.; Elipe, A.; López-Moratalla, T. Non-linear stability of the equilibria in the gravity field of a finite straight segment. *Celest. Mech. Dyn. Astron.* **2001**, *81*, 235–248. [[CrossRef](#)]
18. Blesa, F. Periodic orbits Around simple shaped bodies. *Monogr. Del Semin. Mat. Garcia De Gald.* **2006**, *33*, 67–74.
19. Liu, X.; Baoyin, H.; Ma, X. Periodic orbits in the gravity field of a fixed homogeneous cube. *Astrophys. Space Sci.* **2011**, *334*, 357–364. [[CrossRef](#)]
20. Gabern, F.; Koon, W.S.; Marsden, J.E.; Scheeres, D.J. Binary Asteroid Observation Orbits from a Global Dynamical Perspective. *SIAM J. Appl. Dyn. Syst.* **2006**, *5*, 252–279. [[CrossRef](#)]
21. Zeng, X.; Baoyin, H.; Li, J. Updated rotating mass dipole with oblateness of one primary (I): Equilibria in the equator and their stability. *Astrophys. Space Sci.* **2016**, *361*, 14. [[CrossRef](#)]
22. dos Santos, L.B.T.; de Almeida Prado, A.F.B.; Sanchez, D.M. Lifetime of a spacecraft around a synchronous system of asteroids using a dipole model. *Astrophys. Space Sci.* **2017**, *362*, 202. [[CrossRef](#)]
23. Idrisi, M.J.; Ullah, M.S.; Kumar, V. Elliptic restricted synchronous three-body problem (ERS3BP) with a mass dipole model. *New Astron.* **2021**, *82*, 101449. [[CrossRef](#)]
24. Vincent, A.E.; Tsirogiannis, G.A.; Perdiou, A.E.; Kalantonis, V.S. Equilibrium points and Lyapunov families in the circular restricted three-body problem with an oblate primary and a synchronous rotating dipole secondary: Application to Luhman-16 binary system. *New Astron.* **2024**, *105*, 102108. [[CrossRef](#)]
25. Abozaid, A.; Radwan, M.; Hafez, A.; Bakry, A. Dynamics around small irregularly shaped objects modeled as a mass dipole. *Sci. Rep.* **2024**, *14*, 11764. [[CrossRef](#)]
26. Szebehely, V. *Theory of Orbits. The Restricted Problem of Three Bodies*; Elsevier: Amsterdam, The Netherlands, 1967.
27. McCuskey, S.W. *Introduction to Celestial Mechanics*; Addison-Wesley Publishing Company, Inc.: Reading, MA, USA, 1963.
28. Broucke, R. Traveling between the Lagrange points and the moon. *J. Guid. Control Dyn.* **1979**, *2*, 257–263. [[CrossRef](#)]
29. Roy, A.E.; Ovenden, M.W. On the occurrence of commensurable mean motions in the solar system. The mirror theorem. *Mon. Not. R. Astron. Soc.* **1955**, *115*, 296. [[CrossRef](#)]
30. Roy, A.E. *Orbital Motion*; Routledge: London, UK, 2005.
31. Prado, A.F.B.A. Traveling between the Lagrangian points and the Earth. *Acta Astronaut.* **1996**, *39*, 483–486. [[CrossRef](#)]
32. Cabette, R.E.S.; Prado, A.F.B.A. Transfer orbits to/from the Lagrangian points in the restricted four-body problem. *Acta Astronaut.* **2008**, *63*, 1221–1232. [[CrossRef](#)]
33. Ribeiro, R.S.; de Melo, C.F.; Prado, A.F.B.A. Trajectories Derived from Periodic Orbits around the Lagrangian Point L1 and Lunar Swing-bys: Application in Transfers to near-Earth Asteroids. *Symmetry* **2022**, *14*, 1132. [[CrossRef](#)]
34. Yang, H.; Gong, S.; Baoyin, H. Two-impulse transfer orbits connecting equilibrium points of irregular-shaped asteroids. *Astrophys. Space Sci.* **2015**, *357*, 66. [[CrossRef](#)]
35. Oliveira, G.M.C.; Bertachini de, A. Prado, A.F.; Sanchez, D.M.; Gomes, V.M. Orbital transfers in an asteroid system considering the solar radiation pressure. *Astrophys. Space Sci.* **2017**, *362*, 187. [[CrossRef](#)]
36. Montenbruck, O.; Gill, E. *Satellite Orbits: Models, Methods, and Applications*; Springer: Berlin/Heidelberg, Germany, 2000.
37. Beutler, G. *Methods of Celestial Mechanics, Vol. II: Application to Planetary System, Geodynamics and Satellite Geodesy*; Springer: Berlin/Heidelberg, Germany, 2005.
38. Press, W.H.; Flannery, B.P.; Teukolsky, S.A.; Vetterling, W.T. *Numerical Recipes in C. The Art of Scientific Computing*; Cambridge University Press: New York, NY, USA, 1989.
39. Prado, A.F.B.A. Mapping orbits around the asteroid 2001SN₂₆₃. *Adv. Space Res.* **2014**, *53*, 877–889. [[CrossRef](#)]
40. Sukhanov, A.; Prado, A.F.B.A. Lambert problem solution in the hill model of motion. *Celest. Mech. Dyn. Astron.* **2004**, *90*, 331–354. [[CrossRef](#)]

Disclaimer/Publisher’s Note: The statements, opinions and data contained in all publications are solely those of the individual author(s) and contributor(s) and not of MDPI and/or the editor(s). MDPI and/or the editor(s) disclaim responsibility for any injury to people or property resulting from any ideas, methods, instructions or products referred to in the content.